Korean J. Chem. Eng., **26**(6), 1778-1784 (2009)
DOI: 10.2478/s11814-009-0249-9

Characterization of octadecyltrichlorosilane self-assembled monolayers on silicon (100) surface

Mi-Hee Jung and Ho-Suk Choi†

Department of Chemical Engineering, Chungnam National University, Daejeon 305-764, Korea
(*Received 22 January 2009 • accepted 1 April 2009*)

Abstract−Both monolayers and multilayers were obtained from a dilute solution of *n*-octadecyltrichlorosilane [OTS, $CH_3(CH_2)_{17}SiCl_3$] on a SiO_2/Si surface after a low pressure O_2 plasma treatment. A close-packed monolayer of good quality was formed on the SiO_2/Si surface. The resulting self-assembled layers were characterized by goniometry, atomic force microscopy (AFM), ellipsometry and Fourier transformed infrared attenuated total reflection (FTIR-ATR) spectroscopy. An examination of the time-dependent water contact angle measurements as a function of the OTS concentration revealed rapid monolayer formation at the initial stage. The contact angle measurements showed that the surface structure of the OTS monolayer was quite resistant to environmental changes as a result of the polymerization of OTS molecules and the formation of covalent bonds between the monolayer and substrate surface. The surface was covered with islands (observed by AFM) that were in-filled to produce in a smooth surface. The FRIR-ATR spectra showed symmetric ($\nu s(CH_2)$) and asymmetric ($\nu as(CH_2)$) components perpendicular to the surface.

Key words: n-Octadecyltrichlorosilane, Self Assembled Monolayer, Silane, Silicon

INTRODUCTION

Self assembled monolayers (SAMs) are ordered molecular assemblies formed by the adsorption of an active surfactant on a solid surface. SAMs are generally constructed from amphiphilic molecules with a small head group that has an affinity for the surface and an aliphatic tail. The constituent head and tail groups of amphiphilic molecules make SAMs excellent systems. SAMs can control the chemical and physical properties of a surface, such as wetting, adhesion, lubrication, and corrosion between the surface and interface. Consequently, SAMs have many applications in biology, nanoscience, solid phase catalysts and environmental industry.

There are two representative methods for fabricating SAMs of organic molecules. One is alkanethiols on gold, silver and copper [1,2]. The other is organosilicon on hydroxylated surfaces, such as SiO_2, Al_2O_3, SnO_2, silicate glasses, TiO_2, etc. [3,4]. Thiols are attached by metal-sulfur chemistry where gold is the typical metal of choice to form a thiol SAM, while silanes are adsorbed by silanization on silicon or glass surfaces. The SAMs process and phase behavior of alkanethiols on gold are well understood, which is in contrast to silane-based SAMs on silicon oxide surfaces. Silane-based SAMs are more problematic for both preparation and analysis because the quality of the monolayer is quite sensitive to the reaction conditions, such as the water content, solvent, substrate cleaning, and adsorption temperature. Therefore, various techniques have been used to characterize organosilane monolayers, including contact angle measurements, Fourier transformed infrared attenuated total reflection (FTIR-ATR) spectroscopy, X-ray photoelectron spectroscopy (XPS), ellipsometry, X-ray reflectivity (XRR), grazing incidence X-ray diffraction (GIXD), and atomic force microscopy (AFM). The continuous growth model was derived from XRR and FTIR-ATR, which indicates that a liquid-like, disordered film forms initially, which is converted successively into a highly-ordered final structure with increased coverage [5]. AFM and GIXD studies provide evidence that the submonolayer consists of small islands with a localized structure that is similar to a perfect monolayer, and are separated by uncovered surface regions. With increasing surface coverage, the small islands grow laterally and combine to form larger aggregates until the surface is completely filled with these islands [6].

Fig. 1 shows a schematic representation of the polycondensation

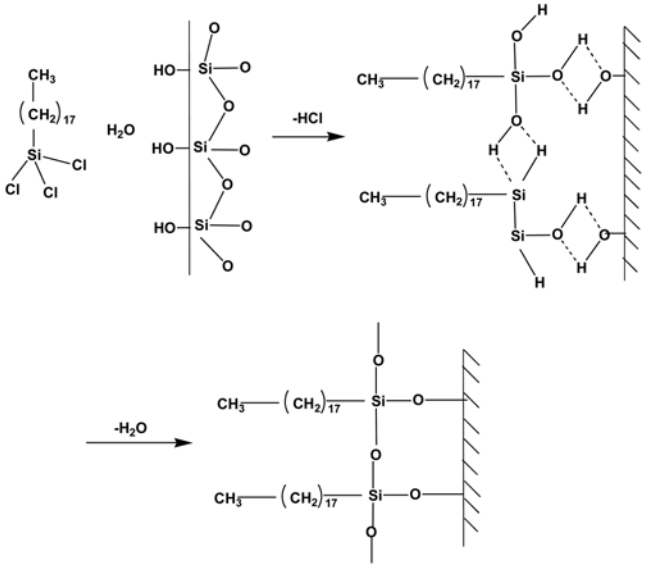

Fig. 1. General scheme proposed for the adsorption of OTS on Si substrates. Note the presence of a thin adsorbed water layer over the SiO_2 surface.

†To whom correspondence should be addressed.
E-mail: hchoi@cnu.ac.kr

and immobilization process of an alkyltrichlorosilane monolayer on a water surface. The chlorine groups of organic silane on the water surface are substituted by hydroxyl groups. The hydroxyl groups in an organic silane molecule react with those in the adjacent molecules and/or with the surface silanol groups. The self assembly of alkylsiloxane on silicon oxide is accommodated by a siloxane linkage to the surface silanol (Si-OH) groups through Si-O-Si bonds or three dimensional condensation by polymerization of the alkyl silanol group. Polymerization of the monolayer and the formation of a covalent bond between the monolayer and substrate enhance the surface stability of the monolayer [7-9].

This study examined the formation of SAMs of the widely used octadecyltrichlorosilane (OTS, (CH_3)-$(CH_2)_{17}$-$SiCl_3$), on the natural silicon oxide surface of a Si(100) wafer. The effect of the adsorbate concentration, immersion time, and solution temperature on the formation of a self assembled OTS monolayer on a silicon substrate was investigated. The monolayer thickness was measured with an ellipsometer. The growth process of the monolayer was examined by using contact angle measurements. The aggregation structure of the monolayers was examined by AFM. The surface chemical composition of the monolayers was investigated by XPS and FTIR-ATR spectroscopy.

EXPERIMENTAL SECTION

1. Substrate Preparation

Commercially available Si(100) wafers were cut into 5×5 mm^2 pieces and cleaned sequentially with trichloroethylene, acetone, and methanol for 5 min at 70 °C in an ultrasonic bath. The samples were rinsed with deionized water and dried with blowing nitrogen. To immobilize the organic silane monolayers on the substrate, the presence of Si-OH groups on the substrate surface is necessary to form a covalent bond between the adsorbate compound and substrate surface. Therefore, an oxygen plasma treatment was performed before deposition of the monolayer. The surfaces were treated with an oxygen low pressure plasma treatment using radio frequency (RF)-generated plasma. The plasma treatment was done at room temperature at 100 W RF power for 3 min. Oxygen gas (flow rate: 10 ml/min) was introduced in the process chamber to activate the surface. The background and processing pressures were 3.0×10^{-2} torr and 4.6×10^{-2} torr, respectively. The oxygen plasma treatment produced a silicon oxide film (SiO_2 thickness: 30 Å) on the silicon surface. After the plasma treatment, the substrates were immersed quickly in deionized water until they were used to prepare the monolayer.

2. Formation of Monolayers

Octadecyltrichlorosilane [OTS, $CH_3(CH_2)_{17}SiCl_3$, purity 90%, Aldrich Co., Ltd] was prepared with a concentration ranging from 2.5×10^{-4} M to 1×10^{-2} M at 299-333 K. The solvent used for the silanization reaction consisted of 80% hexadecane, 12% carbon tetrachloride, and 8% chloroform. OTS was added to the solvent in a nitrogen-filled glove box because the organic silanes react with moisture and polymerize when exposed to air. After adsorption, the OTS-coated samples were washed with chloroform for 30 min in an ultrasonic bath to remove any excess silane deposits, rinsed in deionized (DI) water and then dried with strong blowing nitrogen. Octadecyltrimethoxysilane [OMS, $CH_3(CH_2)_{17}Si(CH_3)_3$, purity 90%, Aldrich Co., Ltd] films were also prepared from a mixture of 80% hexadecane, 12% carbon tetrachloride, and 8% chloroform in a glove box. After adsorption, the surface was treated with the same procedure used for the OTS-coated samples.

3. Analytical Techniques

3-1. Contact Angle Measurements

The contact angle of the substrates was measured by using contact angle goniometry (DSA100, KRÜSS GmbH, Germany) based on static contact angle measurements. A 3 μl drop of the solution was placed on the surface with micropipette. The measurement was performed after the drop had reached "metastable equilibrium" (i.e., the process of spreading stops). The average of at least six measurements was determined. The surface free energy of each surface was calculated from the DI-H_2O and CH_2I_2 data by the Owens-Wendt (OW) method [10]. According to the Owens-Wendt (OW) method, the surface free energy (γ_s) of a solid was defined as the dispersion (γ_s^d) and polar (γ_s^p) components:

$$\gamma_s=\gamma_s^d+\gamma_s^p \tag{1}$$

And it was introduced the following relation:

$$\gamma_{sL}=\gamma_s+\gamma_{Lv}-2[(\gamma_s^d\gamma_L^d)^{0.5}+(\gamma_s^p\gamma_L^p)^{0.5}] \tag{2}$$

Where γ_{sL} is the free energy related to the interface between the solid and the probe liquid, γ_{Lv} is the surface free energy of the liquid, and γ_L^d and γ_L^p are the dispersion and polar components of the surface free energy of the liquid, respectively.

A layer of liquid on a plane solid surface has two interfaces, solid-liquid and liquid-vapor. The balance of tensions at the point of intersection leads to a relationship between the surface tension that is known as Young's equation:

$$\gamma_s=\gamma_{sL}+\gamma_{Lv}\cos\theta \tag{3}$$

When combining Eq. (2) with the Young Eq. (3), the following result is obtained:

$$\gamma_{Lv}(1+\cos\theta)=2[(\gamma_s^d\gamma_L^d)^{0.5}+([(\gamma_s^p\gamma_L^p)^{0.5}] \tag{4}$$

Where θ is the contact angle between the probe liquid and the surface of the tested sample. γ_s^d and γ_s^p in the Eq. (4) can be calculated from the measurements of the contact angle for the surface using by two different liquids with known values of γ_L^d and γ_L^p (Table 1). We used deionized water and methylene diiodide for polar and non polar solvent, respectively.

3-2. Fourier Transformed Infrared Attenuated Total Reflection (FTIR-ATR) Spectroscopy

Table 1. Physical properties of the contact liquids (T_b: boiling point, v: molecular volume, μ: viscosity, χ_p: polarity ($=\gamma_L^p/\gamma_L$), γ_L^d: dispersion component, γ_L^p: polar component, γ_{Lv}: surface free energy)

	H_2O	CH_2I_2
T_b (°C)	100	182
v (nm^3)	0.030	0.130
μ (cP)	1.0	0.5
χ_p	0.70	0.05
γ_L^d (mJ/m^2)	51.0	49.5
γ_L^p (mJ/m^2)	21.8	1.3
γ_{Lv} (mJ/m^2)	72.8	50.8

The infrared spectra were recorded with a Fourier transform infrared spectrophotometer (Model Travel IR, SensIR Technologies) operated at a 2 cm^{-1} resolution with an unpolarized beam striking the sample at normal incidence. The beam diameter was controlled at 6 mm by an aperture placed adjacent to the sample. A Spectra-Tech internal reflection attachment was used for the ATR measurements.

3-3. X-Ray Photoelectron Spectroscopy (XPS)

XPS (ESCA 2000, VG, Micro Tech Co.) was measured by using a Mg*K*a X-ray source (1,253.60 eV) with an emission angle of 15°. The emission angle was defined as the angle between the electron path to the analyzer and the specimen surface. The photoelectrons were collected and analyzed in a concentric hemispherical analyzer by 0000using a fixed analyzer with a transmission energy of 20 eV. The base operating pressure was 7×10^{-9} torr. All the XPS spectra were referenced to the Cls peak (284.6 eV) in order to compensate for any charge-induced shift.

3-4. Atomic Force Microscopy (AFM)

The surface topography and roughness was measured by *ex situ* AFM (PSI, autoprobe CP, USA). A Si tip was used in contact mode in air. The line scanning rates were set to 1.969 Hz. Each image was manipulated with a software program (PSI, version 1.5, USA). With the horizontal direction being the scan direction, all AFM images were background corrected to compensate for the curvature caused by the bending motion of the scanner. The scan images were modified with a polynomial fit to the average height profile in the vertical and horizontal direction.

3-5. Optical Ellipsometry

The average film thickness was measured with a rotating analyzer ellipsometer (Plasmos model SD 2300, New Jersey) equipped with a 632.8 nm He-Ne laser. The angle of incidence was 70°. To determine the effective film thickness, it was assumed that the films were isotropic and homogeneous with a refractive index of 1.465 [11]. The measurements were made at 25 different spots on each sample with a beam spot of 1 mm. The instrumental precision of the ellipsometric angles was 0.04° and the overall, sample-to-sample error in the measurements of the OTS layer thickness was ±0.1 nm. A set of measurements for each substrate was completed within 1 min.

RESULTS AND DISCUSSION

The presence of Si-OH groups on the substrate surface is essential to form a covalent bond between the adsorbate compound and the substrate surface and immobilize the organic silane monolayer on the substrate. The surface was precleaned with solvent. However, the solvent-cleaned surface did not show hydrophilic properties, as shown in Fig. 2(a). Therefore, an oxygen plasma treatment was performed before the monolayer was deposited. The oxygen plasma treatment produced a 35 Å thick oxide film on the surface; the oxide film was identified by XPS. The outer native silicon oxide layer probably terminated with-OH group and was able to serve as the active sites to link alkylsiloxane to the surface of Si(100) wafer via Si-O-Si bonds, which exhibited an almost 0° water contact angle, as shown in Fig. 2(b). The surface became more hydrophobic after immobilizing both OMS (Fig. 2(c)) and OTS (Fig. 2(d)) on the surface. However, when OMS was used as the adsorbate, the surface

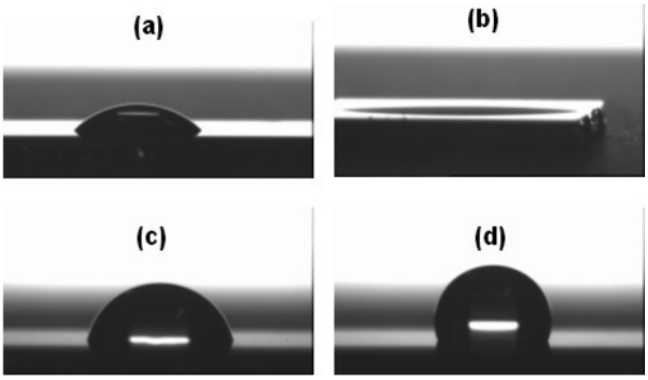

Fig. 2. Side view images of water contact angle on SiO_2/Si substrates. (a) solvent cleaning: contact angle 44°, (b) oxygen plasma treatment: contact angle 1°, (c) octadecyltrimethoxysilane self assembly monolayer: contact angle 81.50°, (d) octadecyltrichlorosilane self assembly monolayer: contact angle 109°.

hydrophobic character was lower than that of the OTS coated sample because there was limited OMS adsorption on the surface. Since three methoxyl groups in OMS create steric hindrance for the OMS to adsorb onto the surface, their contact angle was lower than that of the OTS-coated sample. When the OTS-SAM was formed on the silicon substrate, the contact angle increased to 109° demonstrating the hydrophobic character of the OTS modified Si substrate [12]. The OTS monolayer thickness was measured to be 25 Å with an ellipsometer. This value is similar to 26.5 Å, which is the theoretical OTS molecular length.

Fig. 3 shows the water contact angle for the various concentrations of OTS with increasing immersion time. For all solutions, the contact angles increased rapidly at the initial stage and leveled off. The contact angle increased at a much slower rate once the contact angle approached the expected monolayer (109°). The time required to reach a contact angle of 109° is comparable to that required to achieve the maximum Si-OH concentration in solution. The rate of formation was quite fast at high OTS solution concentrations.

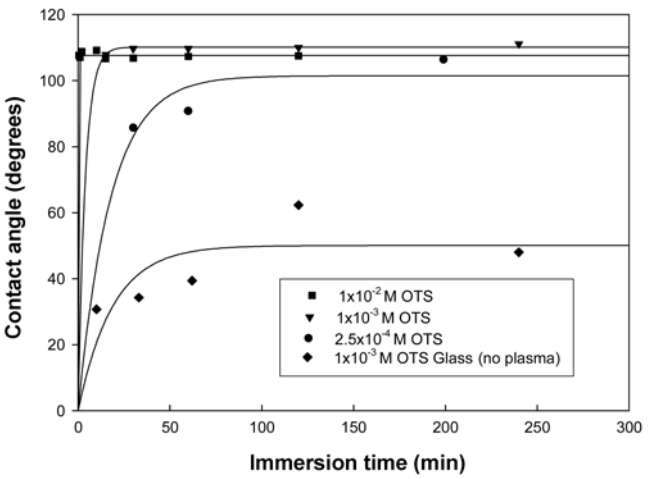

Fig. 3. Rate of formation of an alkysiloxane monolayer prepared from OTS at 26 °C.

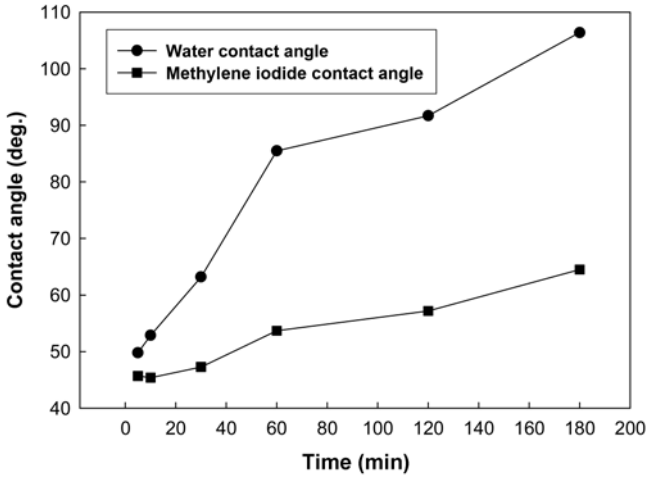

Fig. 4. The contact angles of the SAM coated sample as a function of the immersion time (conditions: OTS concentration 2×10^{-4} M, adsorption temperature 26 °C).

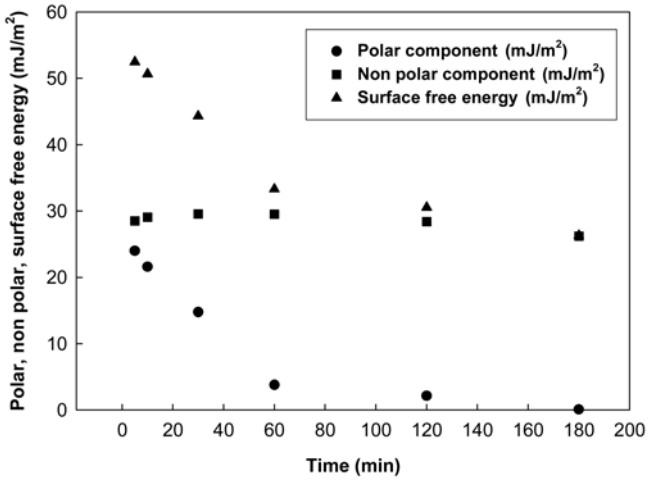

Fig. 5. The surface free energy of the SAM coated sample as a function of the immersion time (conditions: OTS concentration 2×10^{-4} M, adsorption temperature 26 °C).

Both the water contact angle and methylene diiodide contact angle increased with increasing immersion time (Fig. 4). This indicates that the surface had changed to a hydrophobic surface. Fig. 5 shows that the polar component decreased with increasing immersion time because of the consumption of the hydroxyl groups. The coupling silane reactions should be accompanied by a loss of surface water and hydroxyl groups. However, the nonpolar component was constant during the reaction because the alkyl chain of the hydrophobic component does not participate in the polymerization and condensation process. Fig. 5 shows that the polar component was almost zero after 3 h immersion time. After forming a monolayer film, the outer functional group consisted of a nonpolar component (especially -CH=CH_2) [13]. Therefore, the surface free energy originates mainly from the nonpolar component.

Fig. 6 shows the effect of the solution temperature on the adsorption of the silane compound onto the surface. As the preparation temperature was increased, the equilibrium contact angle of the high

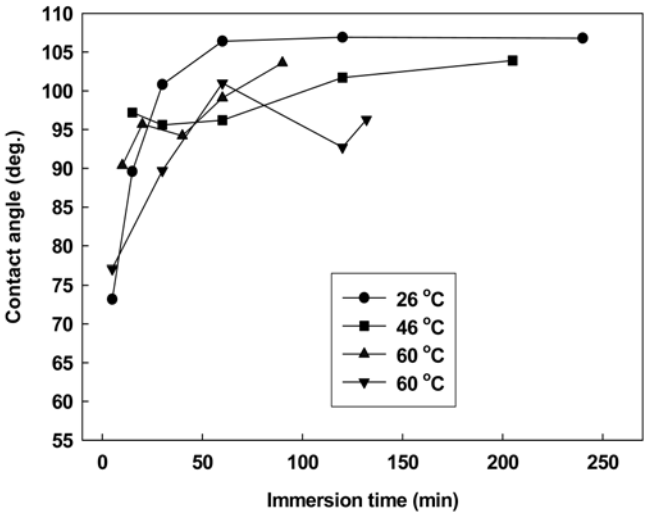

Fig. 6. The solution temperature effect of OTS adsorption rate on the SiO_2/Si surfaces (Conditions: 26 °C (●): 2.5×10^{-4} M OTS, 46 °C (■): 2×10^{-3} M OTS, 60 °C (▲): 1×10^{-3} M OTS. 60 °C (▼): 2.5×10^{-4} M OTS).

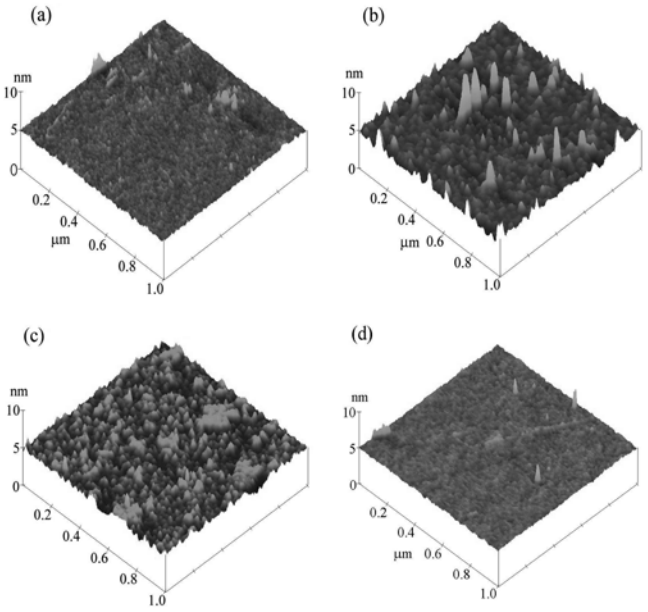

Fig. 7. AFM image of a silane monolayer formed from OTS 2.5×10^{-4} M at 26 °C. (a) immersion time 5 min: RMS roughness 0.15 nm, (b) immersion time 15 min: RMS roughness 0.24 nm, (c) immersion time 30 min: RMS roughness 0.27 nm, (d) immersion time 120 min: RMS roughness 0.11 nm. Image size is 1 μm×1 μm.

temperature film was lower than that of the low temperature film. This means that the wettability was lower on the high temperature film. When the monolayer was prepared below the T_c (approximately 28 °C for OTS), the film exhibited a heterogeneous structure with closely spaced islands of densely packed, almost all-trans alkyl chains arranged perpendicular to the surface. In contrast, when prepared above T_c, the film exhibited a disordered structure with a lower fraction of exposed CH_3 groups and increasing exposure of the wetta-

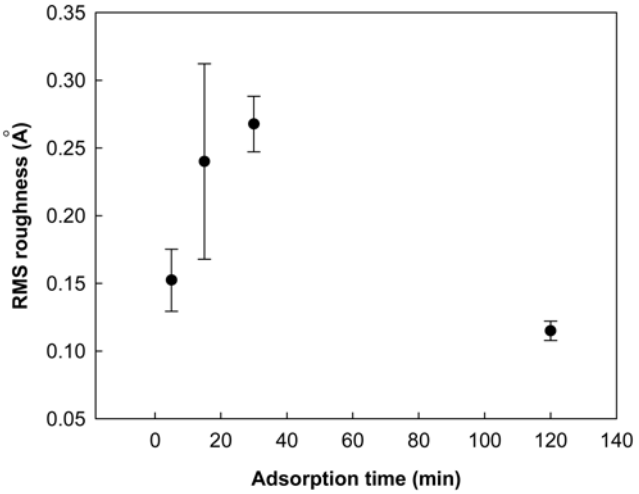

Fig. 8. RMS roughness of a OTS monolayer as a function of the immersion time.

ble surface silanol groups [14].

Fig. 7 shows that the initial surface roughness increased due to the disordered small octadecylsiloxane islands on the surface. As the surface was filled with the aggregation of small islands, the surface roughness decreased with increasing immersion time. Fig. 8 shows that the initial RMS roughness has a large standard deviation from the average RMS roughness. When a complete monolayer was formed, the standard deviation was very small.

Fig. 9 shows typical AFM images on various scales of the surface of a freshly oxidized silicon sample after immersion into a 2.5×10^{-4} M OTS solution in hexadecane for a specified amount of time. In agreement with the previous AFM investigations, bright islands on a darker background, which represent small domains of the final

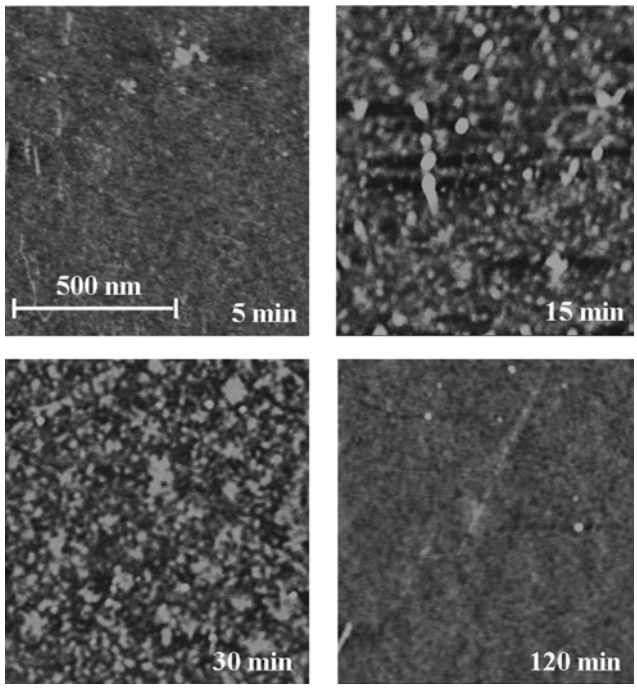

Fig. 9. AFM image series of the surface of freshly oxidized silicon samples after immersion into a 2.5×10^{-4} M OTS for a specified amount of time.

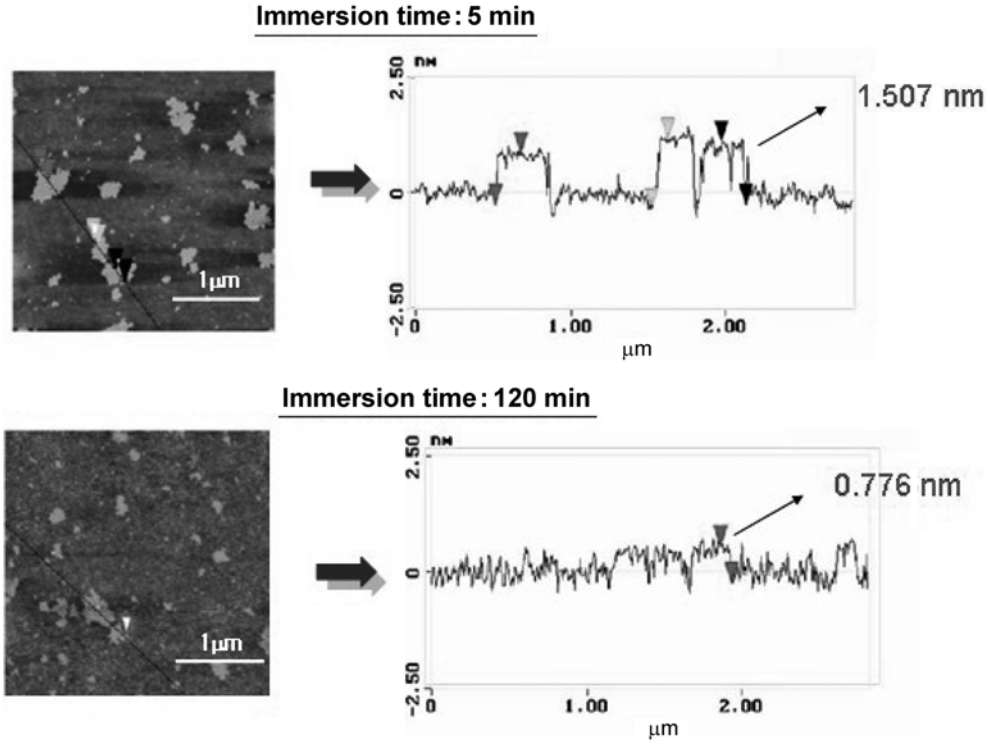

Fig. 10. The AFM image and height profile of incomplete islandlike formation on SiO_2/Si substrates from 2.5×10^{-4} M OTS in solution.

octadecylsiloxane monolayer, can be identified. Schwartz et al. assigned the smaller islands to preorganized polysiloxane assemblies that were constructed in solution prior to adsorption, and the larger islands are aggregates of these assemblies [15]. This is in accordance with the observation of both island types up to a high coverage in this work. The figure shows a series of AFM images of OTS films with increasing immersion time. As can be seen, this increase is caused by the increasing number of OTS islands. A flat surface can be observed after 2 h. This suggests that perfect monolayer coverage is reached after deposition for 2 h [6]. Fig. 10 shows that it is most likely not a good approximation for the 5 min sample because of the sparse coverage. The total thickness of the OTS layer after 5 min was estimated to be 1.507 nm, as is also observed on the larger islands by AFM. After long adsorption times, AFM revealed an apparent decrease in the island height, which is probably caused by the gradual increase in the interstitial areas with increasing density of nonvertically oriented adsorbates [11]. After 2 h, the island height was approximately 0.776 nm.

Fig. 11 shows the XPS spectra of the silicon oxides reacted with OTS at different solution exposure times. All the spectra were scaled to the same total collection time to allow a comparison of the relative intensity. Only a single C1s peak is observed consistently with only a single alkane environment in the molecule (Fig. 11(a)). The intensity of this peak increased with increasing exposure time. The SiO_2 on bare Si substrate surface has a thickness of 3.5 nm. The Si sub-

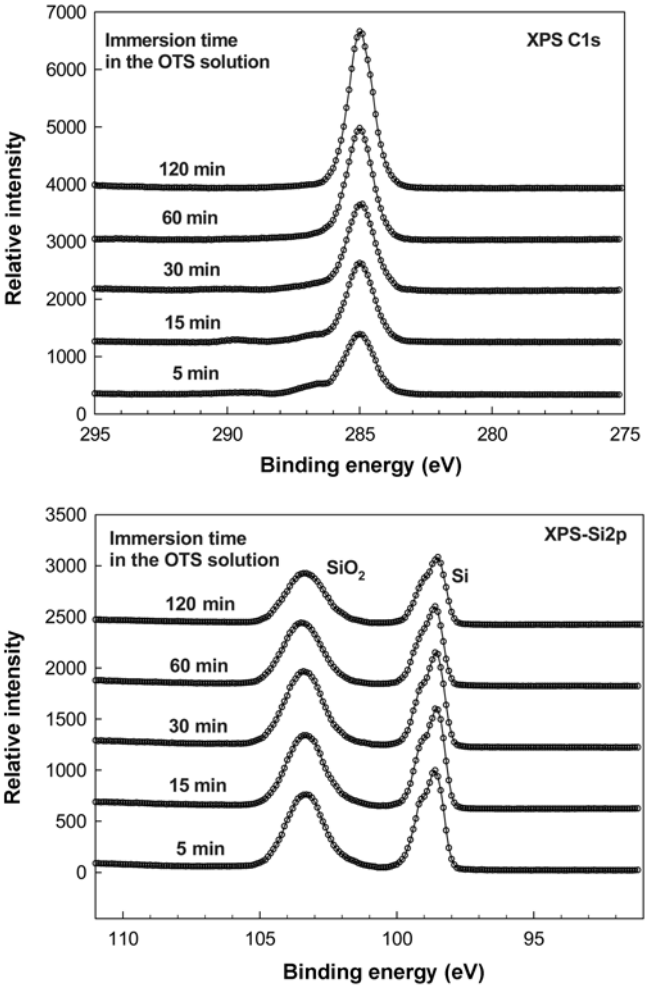

Fig. 11. C(1s) and Si(2p) XPS spectra as a function of the solution (2.5×10^{-4} M OTS) exposure time. All substrates were obtained for the same total data accumulation time.

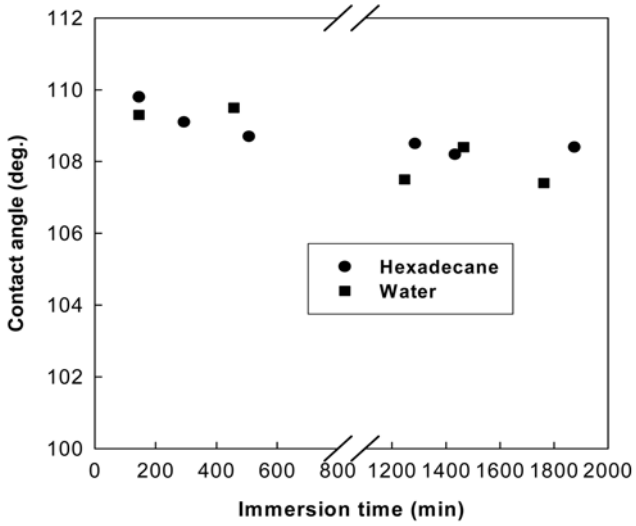

Fig. 12. The stability of the OTS SAM.

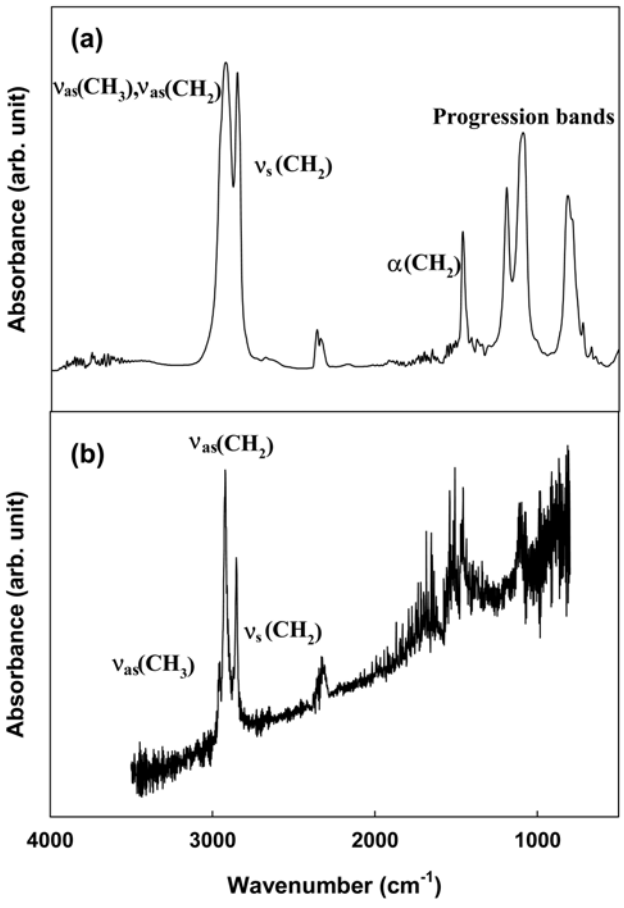

Fig. 13. CH-stretching vibrational mode of (a) FTIR adsorbance spectrum of neat OTS in a KBr capillary cell and (b) FTIR transmission spectrum of an OTS 2-multilayer on silicon.

Table 2. Assignments and positions of the vibrational bands of octadecyltrichlorosilane

Wavenumber (cm^{-1})	Assignment
2,970	$\nu as(CH_3)$
2,930	$\nu as(CH_2)$
2,850	$\nu s(CH_2)$
1,460	$\delta(CH_2)$
1,380-1,250	Progression bands
1,130-1,040	ν (Si-O-Si)
1,010-900	ν (Si-O-Si)

strate showed two peaks in the Si2p binding energy region. One peak at 103.5 eV was assigned to Si(IV) in SiO_2, and the other at 99.5 eV originated from the underlying elemental Si(0) atoms. All spectra showed approximately the same SiO_2/Si ratio (Fig. 11(b)). The peak intensity decreased with increasing exposure time [8].

After immersion in hexadecane/water, Fig. 12 shows that the contact angle of the monolayer is indistinguishable from that determined immediately after preparation. The OTS monolayer shows a good quality, close-packed monolayer on the SiO_2/Si surfaces The contact angle measurements indicate that the surface structure of the OTS monolayer did not reorganize as a response to environmental changes due to polymerization and the formation of a covalent bond between the monolayer and substrate surface.

Fig. 13 shows the transmission spectrum of liquid OTS and ATR-FT-IR spectrum of an OTS 2-multilayer on silicon. Table 2 summarizes the band positions and assignments. The peaks observed at 2,917 and 2,850 cm^{-1} were assigned to the antisymmetric ($\nu as(CH_2)$) and symmetric CH_2 stretching ($\nu s(CH_2)$) bands for the alkyl chain of the OTS molecules, respectively. For the methylene stretching vibrations, $\nu as(CH_2)$ and $\nu s(CH_2)$, the transition dipole moments lie perpendicular to the alkyl chain axis for a fully extended, all-trans alkyl chain. OTS shows a strong and broad Si-O-Si stretching band between 1,130 and 1,040 cm^{-1}, which is in good agreement with other studies [16].

CONCLUSIONS

OTS forms a good quality, close-packed monolayer on SiO_2/Si surfaces. Time-dependent contact angle measurements with water, as a function of the OTS concentration, showed rapid monolayer formation in the initial stage. The contact angle measurements indicated that the surface structure of the OTS monolayer did not reorganize as a response to environmental changes due to polymerization and the formation of a covalent bond between the monolayer and the substrate surface. AFM showed that the surface was covered with islands, which (AFM images) were in-filled to produce a smooth surface. ATR-FT-IR spectroscopy showed that the symmetric ($\nu s(CH_2)$) and asymmetric ($\nu as(CH_2)$) component were perpendicular to the surface.

ACKNOWLEDGMENTS

This work was supported by the Korea Research Foundation Grant funded by the Korean Government (MOEHRD, Basic Research Promotion Fund) (KRF-2008-521-D00083).

REFERENCES

1. C. D. Bain, E. B. Troughton, Y. T. Tao and J. Evall, *J. Am. Chem. Soc.*, **111**, 321 (1989).
2. M. D. Porter, T. B. Bright, D. L. Allara and C. E. D. Chidsey, *J. Am. Chem. Soc*., **109**, 3559 (1987).
3. P. Silberzan, L. Leger, D. Ausserre and J. J. Benattar, *Langmuir*, **7**, 1647 (1991).
4. S. Ge, A. Takahara and T. Kajiyama, *J. Vac. Sci. Technol. A*., **12**(4), 2530 (1994).
5. S. A. Kulkarni, S. A. Mirji, A. B. Mandale, R. P. Gupta and K. P. Vijayamohanan, *Materials Letters*, **59**, 3890 (2005).
6. T. Balgar, R. Bautista, N. Hartmann and E. Hasselbrink, *Surface Science*, **532-535**, 963 (2003).
7. J. B. Brzoska, I. B. Azouz and F. Rondelez, *Langmuir*, **10**, 4367 (1994).
8. R. R. Rye, G. C. Nelson and M. T. Dugger, *Langmuir*, **13**, 2965 (1997).
9. B. C. Bunker, R. W. Carpick, R. A. Assink, M. L. Thomas and M. G Hankins, *Langmuir*, **16**, 7742 (2000).
10. M. Zenkiewicz, *Adhesion Sci. Technol*., **15**, 1769 (2001).
11. N. Rozlosnik, M. C. Gerstenberg and N. B. Larsen, *Langmuir*, **19**, 1182 (2003).
12. P. Jiang, S. Y. Li, H. Sugimura and O. Takai, *Applied Surface Science*, **252**, 4230 (2006).
13. S. R. Wasserman, Y. T. Tao and G. M. Whitesides, *Langmuir*, **5**, 1074 (1989).
14. A. N. Parikh and D. L. Allara, *J. Phys. Chem*., **98**, 7577(1994).
15. D. K. Schwartz, S. Steinberg, J. Israelachvili and J. A. N. Zasadzinski, *Phys. Rev. Lett*., **69**, 3354 (1992).
16. G. Steiner, H. Möller, O. Savchuk, D. Ferse, H. J. Adler and R. Salzer, *J. Mol. Struc*., **563-574**, 273 (2001).